

Data Analogies Enable Efficient Cross-Embodiment Transfer

Jonathan Yang, Chelsea Finn, Dorsa Sadigh
Stanford University

Abstract—Generalist robot policies are trained on demonstrations collected across a wide variety of robots, scenes, and viewpoints. Yet it remains unclear how to best organize and scale such heterogeneous data so that it genuinely improves performance in a given target setting. In this work, we ask: what form of demonstration data is most useful for enabling transfer across robot set-ups? We conduct controlled experiments that vary end-effector morphology, robot platform appearance, and camera perspective, and compare the effects of simply scaling the number of demonstrations against systematically broadening the diversity in different ways. Our simulated experiments show that while perceptual shifts such as viewpoint benefit most from broad diversity, morphology shifts benefit far less from unstructured diversity and instead see the largest gains from data analogies, i.e. paired demonstrations that align scenes, tasks, and/or trajectories across different embodiments. Informed by the simulation results, we improve real-world cross-embodiment transfer success by an average of 22.5% over large-scale, unpaired datasets by changing only the composition of the data.

I. INTRODUCTION

Generalist robot policies are now trained on increasingly large cross-embodiment datasets spanning many robots, morphologies, and viewpoints. At first glance, these results suggest that cross-embodiment learning “just works”—that scaling demonstrations across diverse embodiments naturally enables transfer. Yet the reality is far less clear: we do not know what is actually being transferred when data from other robots is introduced. Current datasets leave critical axes of generalization underrepresented, such as systematic variation in morphology, camera viewpoint, and environment. This raises a key question: are models truly learning useful invariances across morphology and viewpoint, or are their apparent successes merely artifacts of scale? This uncertainty highlights a central gap in the field: we still lack a principled understanding of what kinds of cross-embodiment data actually help a policy adapt to a new robot with only limited data from the target robot setup.

Prior work has largely pursued two strategies for cross-embodiment transfer. Some works simply aggregate demonstrations across robots and environments, banking on diversity at scale to improve robustness [12, 30, 36]. While this more implicit approach to transfer produces strong, consistent gains, it makes the magnitude of true transfer hard to diagnose, leaving it unclear whether the policy’s performance gain is due to direct motion transfer, high-level behavioral transfer, or merely visual regularization. In contrast, explicit alignment methods, such as generative inpainting, offer a way to directly allow demonstrations from one robot in one scene to be used

in another, providing more interpretable assumptions about the mechanism of transfer [9, 23, 24, 31]. However, these methods are less easily scaled, with many assumptions about the scene that fail to scale across the diversity of morphologies and viewpoints in robotics. In this paper, we aim to achieve the best of both worlds: maintaining the scalability of basic data aggregation while achieving the direct, high-fidelity transfer characteristic of explicit alignment methods.

We study how data collection strategies can affect cross-embodiment transfer, when the target robot has only a small amount of collected data. Our investigation considers basic imitation learning on cross-embodiment data, *without* any special architectural or algorithmic changes such as in-painting. While data diversity is known to contribute to generalization, we also consider an orthogonal aspect of the data, which is the degree the data contains analogous data across robot set-ups. These *data analogies* entail demonstrations from different robot embodiments with the similar environments, tasks, and/or trajectories, and have the potential to more explicitly teach the model how different robots relate to each other. See Figure 1 for an example.

The main contribution of this paper is an empirical investigation into how dataset composition impacts cross-embodiment transfer. We focus our experiments on three main aspects of cross-embodiment transfer: camera viewpoint, end-effector morphology, and robot appearance. Our key finding is that data analogies lead to significantly improved transfer compared to simply scaling data diversity, especially for transfer across different morphologies. We observe that our data collection strategy outperforms standard training on large, open-source datasets such as OXE, achieving an average of 19% higher success rate in simulation and 22.5% higher success rate in real-world experiments.

II. RELATED WORKS

The pursuit of generalist robot policies has historically focused on leveraging large, diverse robot datasets [12, 30, 18]. However, policies trained in this manner often failed to generalize to even simple, low-level variations, such as objects of different colors, revealing a critical lack of fundamental visual capabilities. This limitation highlighted the need for a conceptual “glue” to connect low-level actions with high-level semantic understanding. Vision-Language-Action (VLA) models [7, 6, 22, 5, 34, 35, 19, 29] emerged as this glue. By fine-tuning internet-scale vision-language models (VLMs) to predict robot actions, VLAs inherit a rich visual and semantic

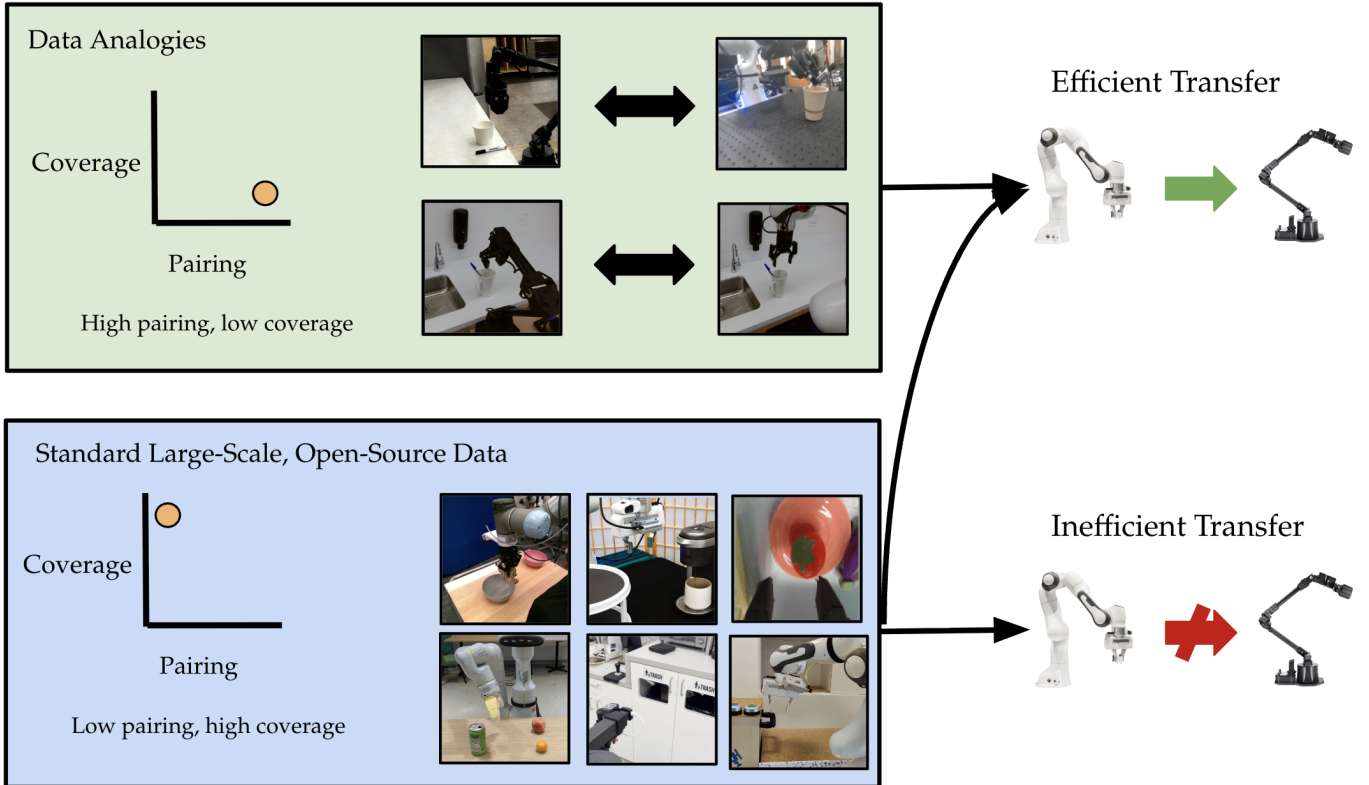


Fig. 1. **Cross-Embodiment Data Analogies.** We study how to collect data so that demonstrations from one robot directly help another. Our data-centric recipe composes breadth (*coverage* across viewpoints, morphologies, and scenes). Then, we search different data scaling strategies to find one that leads to high performance under a fixed budget. We find that datasets with high pairing between scenes and tasks as well as high coverage lead to high transfer performance.

knowledge of the world, which significantly enhances policy generalization and allows them to ingest large-scale, heterogeneous robot datasets [22, 3, 5].

The success of VLAs in learning from diverse, data naturally raised a new question: could policies also leverage data from other robots? Initial findings confirmed that large-scale, cross-embodiment datasets could facilitate transfer [30, 14, 36]. However, it was unclear what type of transfer was occurring or if this highly heterogeneous data was being utilized effectively. This ambiguity sparked two main lines of research: (1) methods that explicitly align data across embodiments, and (2) methods that learn common representations to implicitly bridge the embodiment gap. Explicit alignment methods include generative approaches, such as masking [23, 24, 32] and inpainting robot-specific features [10, 9, 31], as well as motion retargeting [1, 11, 38, 8, 2]. A key drawback of these generative methods is their reliance on assumptions that may not scale, such as the ability to perfectly mask and inpaint novel robot embodiments in arbitrary scenes. Meanwhile, implicit methods focus on learning common representations, often by training large-scale models to project diverse robot data into a shared latent space [40, 39, 13, 31, 36, 26]. These methods offer greater scalability, as they do not require embodiment-specific modules for data translation.

While these model-centric approaches to alignment and

representation have shown promise, they largely treat the underlying data distribution as a given. This overlooks a crucial, emerging direction: focusing on the data distribution itself. For example, recent works have found that carefully collecting and rebalancing data distributions for training VLAs can unlock gains in generalization and transfer [15, 16, 37, 33, 17]. We argue that this data-centric principle is particularly crucial for cross-embodiment learning. Prior works have seen some success in improving robot generalization by expanding the data coverage or diversity of demonstration data [20, 25, 4, 41]. However, it is still unclear what method for scaling are useful to cross the embodiment gap. Analogous to how VLAs provided a high-level glue for generalization, a new data-centric glue is needed to bridge the gaps in embodiment. This work investigates how to scale embodiments by prioritizing the right axes of data coverage and data distribution for high-fidelity cross-embodiment transfer.

III. CROSS-EMBODIMENT DATA ANALOGIES

We consider the problem of transferring behaviors from one or multiple robot embodiments to another embodiment. Zero-shot transfer without any data from the target embodiment is impractically difficult, so we study the few-shot adaptation problem where we have access to a small number of demonstrations from the target embodiment, but where



Fig. 2. **Domain Shift Axes.** We study the role of data diversity and pairing across three domain shift axes: end-effector morphology, camera perspective, and visual appearance.

these demonstrations are not directly for the target task or scenario (e.g. with different objects, skills, or environments than those evaluated on). In this paper, we study how robot data should be collected and organized to enable this form of cross-embodiment generalization. In particular, we find that *data analogies*, or loosely paired demonstrations across embodiments that preserve task-relevant structure despite domain shifts such as viewpoint, end-effector morphology, and appearance, play a central role in enabling effective few-shot cross-embodiment adaptation.

Concretely, we assume a cross-embodiment dataset $\mathcal{D} = \{(e, \tau)\}$, where $e \in \mathcal{E}$ indexes the embodiment (platform, end-effector, viewpoint) and each trajectory τ is a sequence $((o_1^e, a_1^e), \dots, (o_T^e, a_T^e))$. Let e^* denote a target robot with a small few-shot dataset $\mathcal{D}_{e^*}^{\text{few}}$. We start from a pretrained base policy $\pi_{0.5}$ trained on large-scale, generic robot data. Our goal is to use the cross-embodiment dataset \mathcal{D} as a *bridging signal* that exposes the policy to structured variation across embodiments, enabling it to reuse task-relevant structure when adapting to the target robot. Due to computational constraints, we introduce the cross-embodiment dataset \mathcal{D} only during fine-tuning, alongside $\mathcal{D}_{e^*}^{\text{few}}$, to adapt the policy to the target embodiment. Our objective is for the resulting policy π_θ to effectively leverage demonstrations from $e \neq e^*$ to perform the same task on e^* preserving task-relevant structure while adapting embodiment-specific control—under a fixed $\mathcal{D}_{e^*}^{\text{few}}$ budget. Our aim is to identify which data collection strategies enable this form of few-shot cross-embodiment adaptation.

How should we design a data collection strategy that enables effective few-shot cross-embodiment adaptation? We begin by decomposing what a policy must *understand* in order to reuse demonstrations across embodiments. For single-arm manipulators, the cross-embodiment gap is driven by three primary domain shifts: **viewpoint** (camera pose and intrinsics), **end-effector morphology** (gripper geometry and arm kinematics), and **appearance** (textures, lighting, and background). For *each* domain shift, we systematically sweep two orthogonal data collection axes under matched data budgets:

- **Coverage strategy: Targeted vs. Diverse.**

- *Targeted* — Select demonstrations that *close gaps relative to the target robot*, using simple coverage criteria: e.g., fill missing bins in camera extrinsics/intrinsics for *viewpoint*, cover specific gripper types/kinematic regimes for *morphology*, or match scene materials/lighting regimes for *appearance*.
- *Diverse* — Collect broadly varied demonstrations *without target-aware coverage*, sampling viewpoints, morphologies, or appearances uniformly/randomly across what is available.

- **Cross-robot pairing: Unpaired vs. Task-Paired vs. Trajectory-Paired.**

- *Unpaired* — Source and target demonstrations are independent; no cross-robot alignment beyond task labels.
- *Task-Paired* — Demos correspond to the *same task instance* across robots (same objects/initial conditions/goals), but are only *weakly aligned* (e.g., matched hand-designed keypoints).
- *Trajectory-Paired* — A deliberate data collection strategy to capture the *same execution strategy* across embodiments.
 - * **In simulation**, this can be achieved by filtering for demonstrations with highly similar object-centric trajectories via dynamic time-warping (DTW). To make this computational alignment scalable for both real and simulated data, trajectories are first downsampled to a fixed length (50 timesteps).
 - * **In the real world**, this is achieved by collecting demonstrations of the *same task instance* (same scene, objects, and goal) from two different robots, and then computationally aligning the resulting trajectories via DTW.

We aggregate the per-axis strategy datasets into a single *compositional dataset* $\mathcal{D}_{\text{comp}}$, with an equal data budget allocated to each coverage–pairing combination. Across experiments, we find that the most effective data for few-shot cross-embodiment adaptation takes the form of *data analogies*: demonstrations that combine broad coverage across embodiments with strong, trajectory-level pairing that preserves task-relevant structure over time. These paired analogies enable the policy to meaningfully reuse cross-robot demonstrations, rather than treating embodiment variation as unstructured noise.

IV. EXPERIMENTS

Our goal is to evaluate *cross-embodiment translation*: can demonstrations collected on one robot help a different robot perform the *same* task with only a few target examples? We align our study around four questions that map directly to the four main figures.

- 1) **Q1 (Fig. 1): Under a fixed budget, what data collection strategy leads to the highest performance for each generalization axis?**

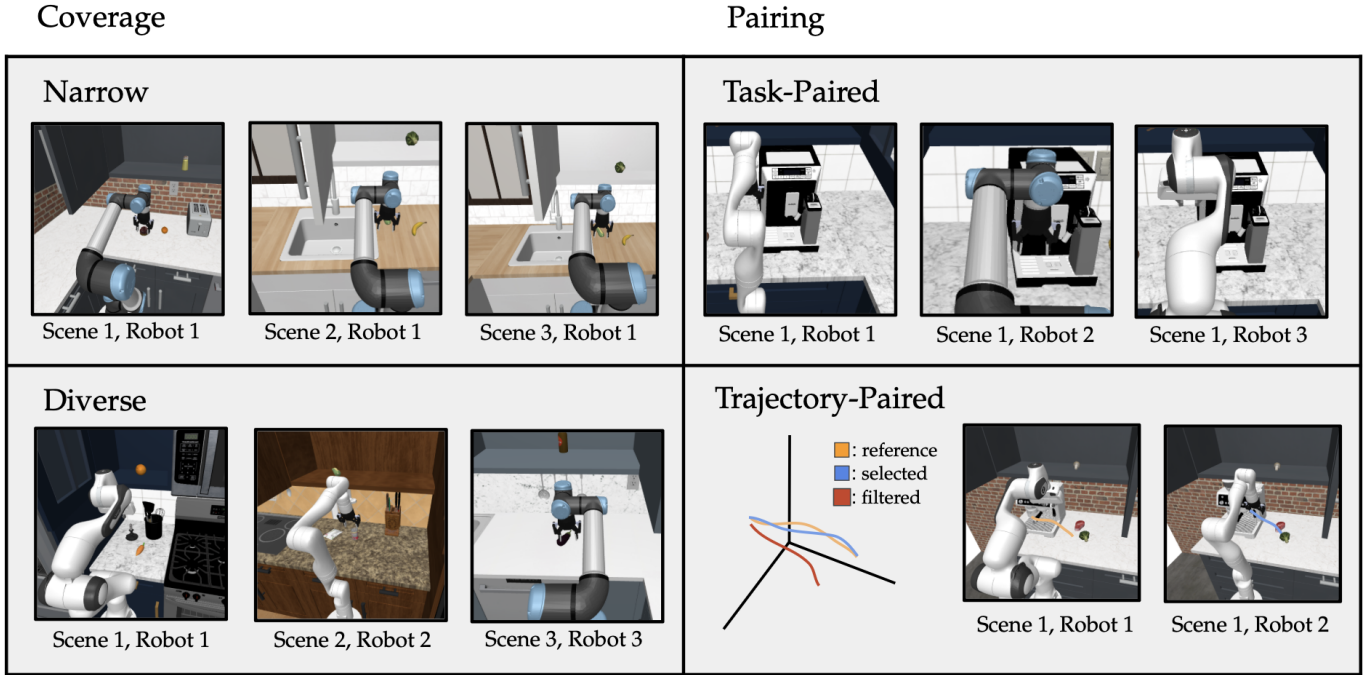


Fig. 3. **Coverage versus Pairing.** Simulation images depicting the data collection strategies. Coverage is the diversity of data on the generalization axis, while pairing is the similarity of the tasks or trajectories in the data.

- 2) **Q2 (Fig. 2):** How does our compositional data-collection strategy from Q1 compare to naively training on large open-source datasets?
- 3) **Q3 (Fig. 3):** How does translation improve as we scale the diversity of source data?
- 4) **Q4 (Fig. 4):** Do these trends hold on real robots (PiperX, WidowX, Franka, Piper)?

Simulation Environment

We use a RoboCasa-based benchmark for cross-embodiment learning [28]. Tasks: *PnP Counter*→*Sink*, *PnP Sink*→*Counter*, *Turn On Sink Faucet*, and *Flip Mug Upright*, where “PnP” stands for “Pick and Place”. Scenes vary kitchen layout, textures, objects, and camera placement. Priors are generated with MimicGen [27] for three embodiments (Kinova, Kinova3, UR5e) with Robotiq 2F-85/2F-140 grippers. In order to ensure that the simulation resets to the same state, we standardize the environment generation seed across experiments. This allows us to

Real-World Environment

We evaluate on three targets: **Franka**, **WidowX**, and **PiperX** (parallel-jaw). For each experiment, we collect 50 demonstrations on the robot we want to transfer from. Then, we use our translational dataset collected as described below with 50 demonstrations per axis, scene, and robot.

Experiment Setup

Policy and Inputs. We use a vision–language–action policy (VLA, $\pi_{0.5}$ -style) $\pi_{\theta}(a_t | o_{1:t}, e, \ell)$ with an embodiment token

e and language task prompt ℓ , where actions are represented in joint space. The policy is instantiated with $\pi_{0.5}$: a vision–language backbone that embeds the history of observations and language into tokens, followed by a flow-matching action expert that predicts a short-horizon sequence of joint actions. Concretely, we encode the third-person and wrist RGB images, proprioceptive state, embodiment token e , and text prompt ℓ into a sequence of tokens, append learned action tokens corresponding to a horizon- $H = 20$ sequence of joint position (or velocity/torque) commands, and process the resulting sequence with a small transformer. During training, we corrupt the ground-truth joint action sequence $a_{t:t+H-1}$ with Gaussian noise at a randomly sampled diffusion timestep and train the network to predict this noise, as in standard diffusion policies; at test time, we sample from the learned reverse process and execute only the first joint action a_t .

Training. We start with the base $\pi_{0.5}$ VLA with pretrained weights [18], then *co-fine-tune* on the union of target few-shot demonstrations and a selected subset of source data, known as the “translation dataset” according to each study condition. Unless otherwise noted, we combine target and translation dataset at a 50:50 ratio within each mini-batch. For the target-only and target upper-bound baselines, we finetune only with data from the robot we want to transfer from, or the robot we want to transfer to. Fine-tuning takes around 8 hours on an NVIDIA A100 40GB GPU. Crucially, we do not modify the model architecture, loss functions, or optimization procedure; all experiments share the same training setup. Our study isolates the effect of *data composition* during fine-tuning.

Translation Data Collection. The translation dataset is

constructed by systematically addressing each domain shift axis using the appropriate coverage and pairing strategy as determined by our ablation studies (Fig. 11). *In simulation*, for the *viewpoint* axis, we leverage RoboCasa’s procedural generation to sample diverse camera poses and intrinsics via changing the azimuth, elevation, and focal length. For the *morphology* axis, we collect demonstrations across three robot platforms (Franka Emika Panda, Kinova3, UR5e) with different gripper types (Robotiq 2F-85/2F-140) using targeted coverage to span kinematic regimes and workspace geometries relevant to the target robot, with trajectory pairing obtained by filtering MimicGen-generated priors for high DTW similarity in end-effector and object keypoint trajectories. For the *appearance* axis, we use RoboCasa’s texture randomization to diversely vary kitchen materials, lighting, and object appearances.

In the real world, for diversity in *viewpoint* and *morphology*, we vary the third-person camera and use the corresponding end-effectors. For *appearance*, we augment the datasets with inpainted robots to the buffer using Dall-E 3. We keep the environment and state the same, only replacing the texture of the robot. Note that this process is a bit noisy, and sometimes textures that are not part of the robot get inpainted. However, in practice, these errors seem minimal as the model has qualitatively good performance.

Data Budget. Unless otherwise stated, we use a fixed budget of **50 demonstrations per (robot, task)** combination for both translational data (or data that is included during co-finetuning to help the policy to understand cross-embodiment correspondences) and targets (data from another robot that we want to transfer). We report two references in every plot: *Target-only* (few-shot baseline with no source data) and *Target upper bound* (spending the same extra budget on the target robot). The results are compiled over random initializations 5 in the real-world and random seeds 100 in simulation.

Compositional data mixture (OXE+Translational). For experiments that use *OXE+Translational* (Fig. 6, Fig. 8), the *source* half of each co-fine-tuning batch is drawn as 60% *OXE* (unpaired) and 40% *Trajectory-Paired*. Within the *OXE* pool, we reweight sampling to flatten histograms along viewpoint (camera azimuth/elevation bins) and morphology (gripper/kinematic class), avoiding over-representation of a few robots or camera setups. Across conditions, we fix the number of *source* samples seen per epoch to isolate the effect of pairing versus volume.

Data Selection Methods. We instantiate four selection strategies that factor coverage and pairing:

- *Uniform (Naïve scaling)*: uniformly sample source demos across embodiments.
- *Targeted coverage*: select source demos to fill gaps in *viewpoint* (camera pose/intrinsics) and *morphology* (gripper/kinematics) relative to the target’s few-shot set; appearance diversity is secondary.
- *Task-Paired*: for each target task instance, include source demos of the *same task* (same objects/goals).
- *Trajectory-Paired*:
 - *Simulation*: For each trajectory, we select a coun-

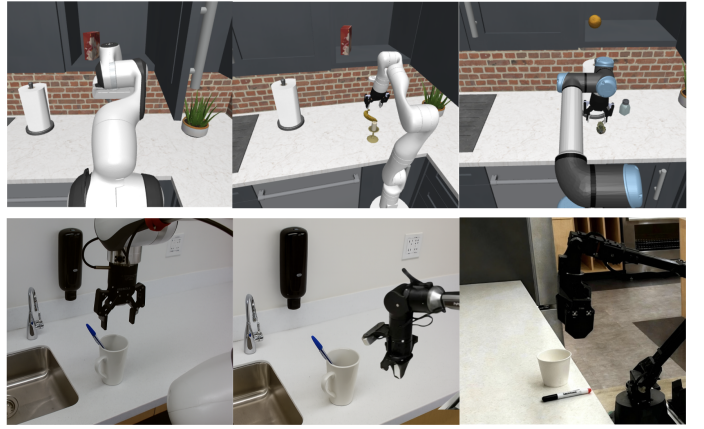


Fig. 4. **Sim and Real-World Robots.** We train a *cross-embodiment* policy to transfer the tasks of putting a pen in a cup and putting a book on a bookshelf to a new robot. We evaluate with the Franka Emika Panda, WidowX, and ARX Piper robot arms.

terpart by comparing proprioceptive features (end-effector pose, gripper state) and object keypoints. We define a task-specific *event keypoint* t^* (e.g., first stable grasp) and align the approach segments (start $\rightarrow t^*$) across trajectories using dynamic time warping (DTW) over a task-space feature $\phi_t = [x_t^{ee}, R_t^{ee}, g_t, \kappa_t]$, where κ_t is an object-centric progress scalar (distance to the nearest task-relevant object keypoint in the object frame). Trajectories are downsampled to a fixed length (50 timesteps). The nearest neighbor under the DTW cost is chosen as the paired trajectory.

- *Real World*: We collect demonstrations from different robots (e.g., a WidowX and a Franka) in the same task instance (same objects, layout, and goal) and then align them with DTW on ϕ_t . In practice, the “identical scene” criterion means the same staged setup with matched object placements and camera viewpoints within normal lab tolerances; no special fiducials are required.

A. *Under a fixed budget, what data collection strategy leads to the highest performance for each generalization axis?*

Figure 11 compares success across *viewpoint*, *morphology*, and *appearance* under matched source budgets. In all settings, the target robot contributes only **50** demonstrations; we pre-train on sources and co-fine-tune on the union of this 50-shot target set and a selected subset of source data. Bars report means over 3–5 seeds for a fixed VLA trained with distinct *coverage* (targeted vs. diverse) and *pairing* (unpaired, task-paired, trajectory-paired) choices; dashed lines mark the *Target-only* baseline and a *Target upper bound* that spends the same extra budget directly on the target.

Diversity helps for viewpoint and appearance. For shifts dominated by perception—camera pose/intrinsics (*viewpoint*) and scene/textures (*appearance*)—*diverse* coverage outperforms *targeted* at a fixed pairing level. Broad visual varia-

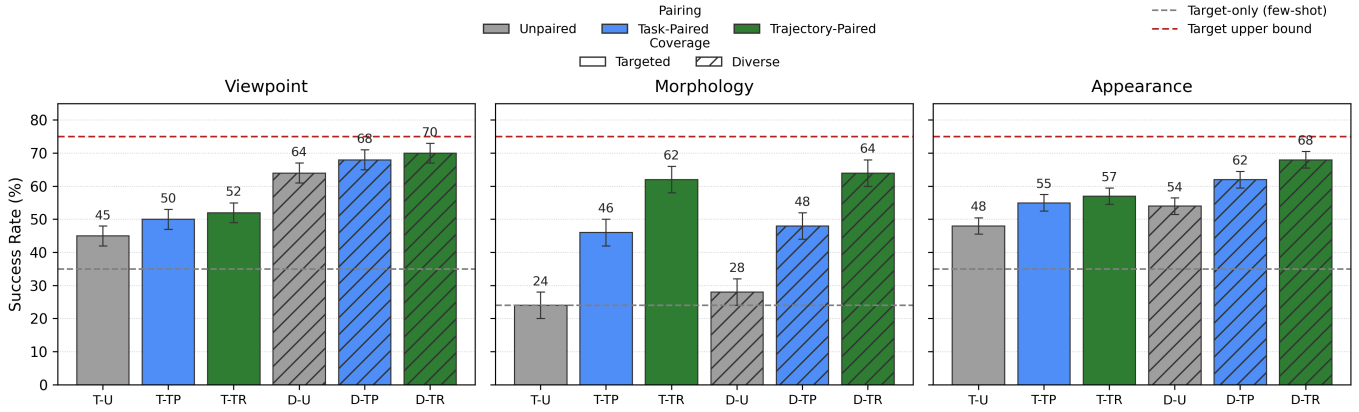


Fig. 5. **Main coverage plot (Success Rate).** Success Rate (%) on the target robot across Coverage×Pairing for (a) Viewpoint, (b) Morphology, (c) Appearance. Error bars: 95% CI. Dashed lines show Target-only (few-shot) and Target upper bound (same extra budget on target).

tion regularizes the encoder, reduces overfitting to scene- or camera-specific cues, and improves generalization even with weak alignment. In practice, sampling many camera poses, lighting regimes, and backgrounds produces larger gains than narrowly matching the target’s exact settings.

Targeted coverage is more effective for morphology. When the distribution shift involves morphology, targeted selection provides a larger advantage than purely diverse sampling. As shown in Figure 11, performance along the morphology axis is similar for targeted and diverse selection (62% vs. 64% for T-TR and D-TR), but the gap between paired and unpaired settings is substantially larger, averaging 23%. We hypothesize that this effect arises because different morphologies demand different object-manipulation strategies.

B. How does our compositional data-collection strategy from Q1 compare to naively training on large open-source datasets?

Figure 6 compares our compositional dataset design against training directly on large, unpaired open-source data. While large datasets such as OXE contain extensive demonstrations across robots and scenes, they are overwhelmingly *unpaired* and emphasize scale over structure. We evaluate whether reweighting data coverage and introducing explicit translational pairs can outperform pure data volume.

OXE is a strong baseline in simulation, but pairing leads to higher performance In Figure 6, we compare our method against *Baseline*, *Narrow*, and *OXE*. For *Narrow* and *OXE*, the translation dataset is replaced by the corresponding datasets (i.e., they are sampled as 50% of each finetuning minibatch). While OXE provides a strong improvement over narrow paired data, our method consistently outperforms OXE across all tasks and both target robots, achieving an average of 19% **higher success rate**. These gains are most pronounced on contact-rich tasks, indicating that explicit pairing and alignment are critical for fully leveraging large, unpaired datasets. This supports the view that while diversity at scale helps, explicit correspondences are a critical component to ensure that the morphology domain gap is crossed.

Structured diversity is a valuable first step, but its gains are limited without explicit pairing. The results also show that simply using a more diverse, structured data pool (*OXE*) improves over a narrow, two-robot baseline (*Bridge+DROID*), validating that broader coverage of cameras and scenes helps generalization. However, these gains from diversity alone plateau and are surpassed across tasks by our *OXE+Translational* method. One contributing factor in simulation is that OXE’s real-world visual diversity does not perfectly align with simulated image statistics, limiting perception regularization. Our work points to a data-scaling path that emphasizes composition—more pairing, broader coverage, and structured diversity—over simple aggregation.

Our compositional dataset differs from large unpaired sources along two key dimensions: (1) it *balances coverage* across morphology and viewpoint axes to avoid overrepresentation of a few robots or camera setups, and (2) it *injects trajectory-level pairing* between related embodiments, encouraging policies to learn embodiment-invariant task representations. By ensuring that the domain gap is crossed for each axis, our method leads to significantly greater generalization than using unpaired data. In short, even under fixed budgets, scaling data *structure on top of* scaling data *volume* delivers the best results: carefully composed cross-embodiment collections consistently add gains over strong unpaired baselines.

C. How does translation improve as we scale the diversity of source data?

Viewpoint and appearance scale smoothly with diversity. For *viewpoint* and *appearance*, increasing diversity produces predictable, steady improvements across methods: adding more camera configurations and scene variations consistently lifts performance (an average increase of 17%). One plausible explanation is that broader coverage reduces distribution shift between source and target settings, making it more likely that the target’s conditions are represented during training. Notably, the success rate of *trajectory pairing* maintains a consistent advantage even as diversity grows, by an average of 6% over

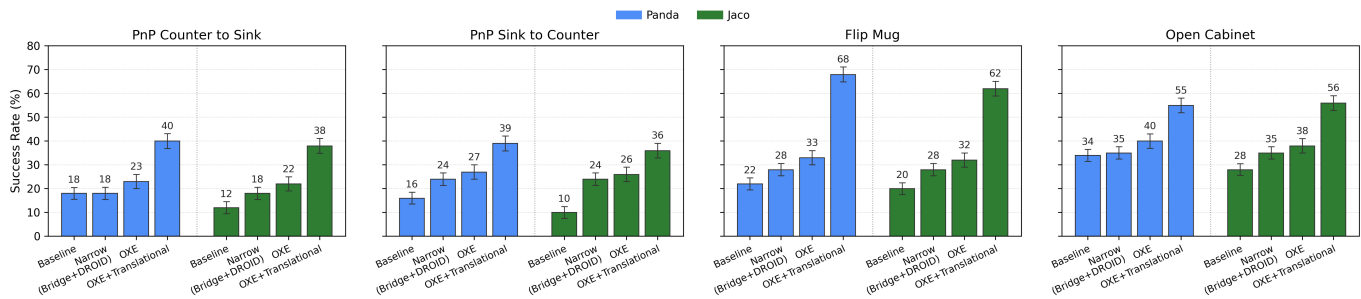


Fig. 6. **Comparison with large open-source datasets.** Success Rate (%) on four RoboCasa tasks when training on (i) narrow two-robot data (*Bridge+DROID*), (ii) large unpaired open-source datasets (*OXE*), and (iii) our *OXE+Translational* composition that reweights coverage and adds trajectory-level alignment. Results are shown for two target robots (**Panda**, **Jaco**); error bars denote 95% CI.

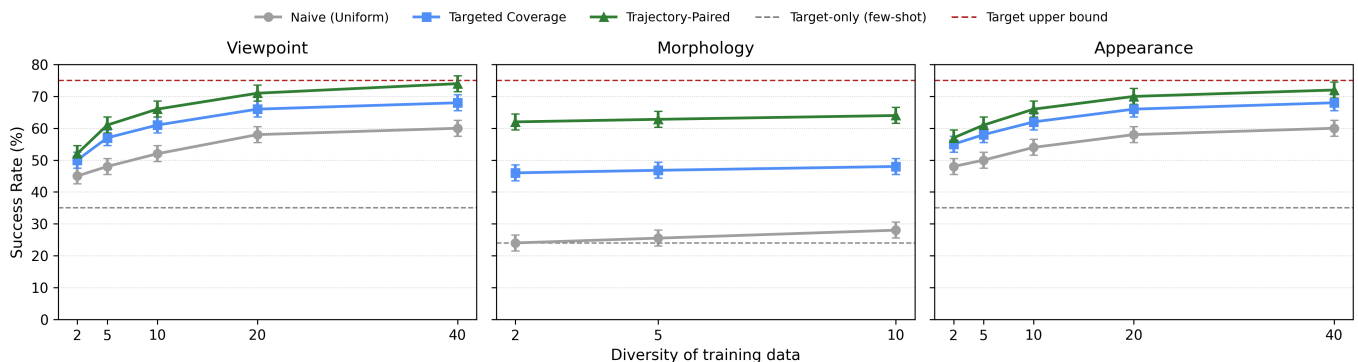


Fig. 7. **Effect of scaling diversity.** Success Rate (%) on the target robot as we increase the diversity of source data (distinct embodiments, viewpoints, and scenes). Curves compare *Naive/Uniform*, *Targeted Coverage*, and *Trajectory-Paired*. Dashed lines show the 50-shot *Target-only* baseline and the *Target upper bound*.

its less-paired counterpart—suggesting that aligning sequences across instances helps the model use this additional coverage more effectively rather than treating it as unrelated samples.

Morphology saturates without pairing. On the *morphology* axis, our results show that simply increasing the diversity of end-effectors does not enable generalization to new morphologies. Instead, strong cross-robot pairing is the dominant factor. This is evident in the data: increasing diversity (whether *uniform* or *targeted*) barely moves the performance curves (42% \rightarrow 44%). Adding more arms or grippers without correspondences fails to resolve action-scale and kinematic mismatches; the policy sees different control distributions that cannot be reconciled by visual breadth alone. Temporal pairing, however, injects an object-frame alignment that effectively “translates” motion primitives across embodiments, converting cross-robot data into usable control supervision.

While data diversity solves the visual perception challenge—widening what the model can see and governing perception-level robustness—it is insufficient for action-level transfer. Instead, methods that encourage more correspondences between the two robots, such as task-paired or, more effectively, trajectory-paired data collection, are required. This “connectivity” provides the critical link that specifies how observations *should* map to actions on a different robot.

D. Do these trends hold on real robots (Franka, WidowX, Piper)?

On real hardware, the benefits of translation data become more pronounced. Figure 8 shows that the progression observed in simulation carries over to real robots: moving from a few-shot baseline to a narrow two-robot pool helps, reweighting large open-source data toward broader coverage helps more, and composing that pool with explicit cross-robot pairs delivers the largest improvements. Across embodiment settings that include both cross-platform transfer (PiperX \rightarrow WidowX, WidowX \rightarrow Franka) and a morphology change (WidowX \rightarrow Piper), *OXE+Translational* improves success by an average of 25% over *OXE*. This indicates that the benefits of cross-embodiment pairing are not simulator-specific. Instead, in the real-world, targeted data collection is even more necessary in order to cross the morphology gap between robots.

Our translation dataset allows for transfer of tasks from existing open-source datasets. Figure 9 depicts transfer results on two BRIDGE tasks, *Strawberry in Pot* and *Stack Red Block on Blue*. In order to test generalization to new scenes and avoid potential dataset leakage from the pretraining dataset of $\pi_{0.5}$, we evaluate each policy in two held-out real-world environments: a toy kitchen setup and a visually distinct wooden table setup. Notably, policies trained solely on BRIDGE fail to transfer, achieving 0% success across

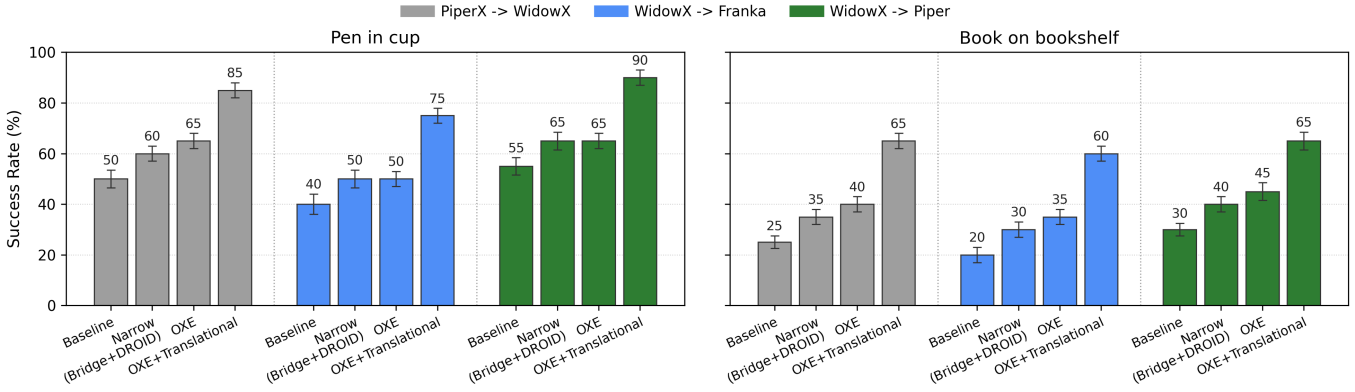


Fig. 8. **Real-robot transfer.** Success Rate (%) on two tabletop tasks under three embodiment settings: PiperX \rightarrow WidowX, WidowX \rightarrow Franka, and WidowX \rightarrow Piper. Bars compare a few-shot target baseline, a narrow two-robot pool (*Bridge+DROID*), a diversity-weighted open-source pool (*OXE*), and our composed *OXE+Translational*. Error bars denote 95% CI.

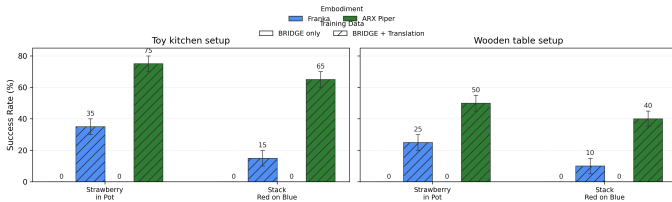


Fig. 9. **BRIDGE dataset transfer.** We evaluate how well our method leads to transfer on two BRIDGE tasks across two environments each.

all embodiments, tasks, and environments. However, when BRIDGE is augmented with paired translation data, cross-embodiment transfer performance is much higher.

For simpler manipulation behaviors that closely resemble motions present in the translation dataset—such as pick-and-place actions in *Strawberry in Pot*—transfer performance is high, reaching up to 75% success in the toy kitchen and 50% on the wooden table. In contrast, more precision-sensitive behaviors such as block stacking exhibit lower, but still non-zero, success rates, improving from 0% to as high as 65% in the toy kitchen and 40% on the wooden table. Performance consistently degrades in the wooden table setup, reflecting the added challenge of visual and geometric scene shifts. Overall, these results indicate that while large open-source datasets are not directly reusable across embodiments, a small amount of targeted translation data can unlock substantial transfer, particularly for manipulation skills that tolerate moderate spatial imprecision.

There is substantial headroom in how we scale robot data. These hardware results suggest that cross-embodiment transfer can be significantly improved by adding more structure to the data collection process. Rebalancing coverage across viewpoint and morphology already yields reliable gains over narrow pools, and introducing even modest amounts of cross-robot pairing correlates with further, repeatable improvements without collecting dramatically more demonstrations. In practice, this points to a concrete path for future datasets: allocate budget toward (i) diversity to cross the visual gap be-

tween robots and (ii) correspondences between embodiments. The consistent boosts on physical systems indicate that better-curated collections could unlock substantially stronger cross-robot generalization than current unpaired corpora afford.

V. CONCLUSION

By systematically varying viewpoint, morphology, and appearance under matched budgets, three design principles emerge. *First*, breadth helps chiefly where variation is perceptual: increasing diversity in camera and scene coverage yields steady gains for viewpoint and appearance. *Second*, morphology—the axis that changes how actions must be executed—benefits most from *targeted* coverage. *Third*, and most importantly, *pairing* leads to large transfer benefits: introducing cross-robot correspondences consistently adds gains on top of strong unpaired baselines. Rather than accumulating more isolated islands of demonstrations, it is important to balance coverage along morphology and viewpoint, and invest a portion of budget in pairing that anchors examples in a common frame.

VI. LIMITATIONS

While our results show consistent gains from structured coverage and trajectory pairing, our study has several limitations. First, conclusions are drawn using a $\pi_{0.5}$ -style VLA under a fixed few-shot budget; other architectures, larger budgets, or alternative training recipes could shift absolute performance and sometimes the relative gaps. Second, dataset shift remains: OXE and our scenes differ from simulation distributions and from other labs; our compositional strategy may require retuning to new object distributions, sensors, and embodiments. Finally, while our study drew conclusions from diverse simulations, the scope of experiments were within two buildings for the real world. This means that it is unclear to what extent the translation dataset should scale to provide consistent general transfer between two real robots.

VII. ACKNOWLEDGEMENTS

This work was supported in part by the Defense Advanced Research Projects Agency (DARPA) and the Toyota Research Institute (TRI). This material is also supported by the National Science Foundation under Grant No. 2125511.

REFERENCES

- [1] Kfir Aberman, Peizhuo Li, Dani Lischinski, Olga Sorkine-Hornung, Daniel Cohen-Or, and Baoquan Chen. Skeleton-aware networks for deep motion retargeting. *ACM Transactions on Graphics*, 39(4), August 2020. ISSN 1557-7368. doi: 10.1145/3386569.3392462. URL <http://dx.doi.org/10.1145/3386569.3392462>.
- [2] Sai Haneesh Allu, Jishnu Jaykumar P, Ninad Khargonkar, Tyler Summers, Jian Yao, and Yu Xiang. Hrt1: One-shot human-to-robot trajectory transfer for mobile manipulation, 2025. URL <https://arxiv.org/abs/2510.21026>.
- [3] Suneel Belkhale and Dorsa Sadigh. MiniVLA: A Better VLA with a Smaller Footprint, 2024. URL <https://github.com/Stanford-ILIAD/openvla-mini>.
- [4] Hongzhe Bi, Lingxuan Wu, Tianwei Lin, Hengkai Tan, Zhizhong Su, Hang Su, and Jun Zhu. H-rdt: Human manipulation enhanced bimanual robotic manipulation, 2025. URL <https://arxiv.org/abs/2507.23523>.
- [5] Kevin Black, Noah Brown, Danny Driess, Adnan Esmail, Michael Equi, Chelsea Finn, Niccolo Fusai, Lachy Groom, Karol Hausman, Brian Ichter, et al. π_0 : A Vision-Language-Action Flow Model for General Robot Control. In *Proceedings of Robotics: Science and Systems (RSS)*, 2025.
- [6] Anthony Brohan, Noah Brown, Justice Carbajal, Yevgen Chebotar, Xi Chen, Krzysztof Choromanski, et al. RT-2: Vision-Language-Action Models Transfer Web Knowledge to Robotic Control. In *Conference on Robot Learning (CoRL)*, 2023.
- [7] Anthony Brohan, Noah Brown, Justice Carbajal, Yevgen Chebotar, Joseph Dabis, Chelsea Finn, et al. RT-1: Robotics Transformer for Real-World Control at Scale. In *Proceedings of Robotics: Science and Systems (RSS)*, 2023.
- [8] Zhefeng Cao, Ben Liu, Sen Li, Wei Zhang, and Hua Chen. G-dream: Graph-conditioned diffusion retargeting across multiple embodiments, 2025. URL <https://arxiv.org/abs/2505.20857>.
- [9] Lawrence Yunliang Chen, Kush Hari, Karthik Dharmarajan, Chenfeng Xu, Quan Vuong, and Ken Goldberg. Mirage: Cross-embodiment zero-shot policy transfer with cross-painting, 2024. URL <https://arxiv.org/abs/2402.19249>.
- [10] Lawrence Yunliang Chen, Chenfeng Xu, Karthik Dharmarajan, Muhammad Zubair Irshad, Richard Cheng, Kurt Keutzer, Masayoshi Tomizuka, Quan Vuong, and Ken Goldberg. Rovi-aug: Robot and viewpoint augmentation for cross-embodiment robot learning, 2024. URL <https://arxiv.org/abs/2409.03403>.
- [11] Sungjoon Choi, Min Jae Song, Hyemin Ahn, and Joohyung Kim. Self-supervised motion retargeting with safety guarantee, 2021. URL <https://arxiv.org/abs/2103.06447>.
- [12] Sudeep Dasari, Frederik Ebert, Stephen Tian, Suraj Nair, Bernadette Bucher, Karl Schmeckpeper, Siddharth Singh,

- Sergey Levine, and Chelsea Finn. RoboNet: Large-Scale Multi-Robot Learning. In *Conference on Robot Learning (CoRL)*, 2019.
- [13] Ria Doshi, Homer Walke, Oier Mees, Sudeep Dasari, and Sergey Levine. Scaling Cross-Embodied Learning: One Policy for Manipulation, Navigation, Locomotion and Aviation, 2024.
- [14] Ria Doshi, Homer Walke, Oier Mees, Sudeep Dasari, and Sergey Levine. Scaling cross-embodied learning: One policy for manipulation, navigation, locomotion and aviation, 2024. URL <https://arxiv.org/abs/2408.11812>.
- [15] Jensen Gao, Annie Xie, Ted Xiao, Chelsea Finn, and Dorsa Sadigh. Efficient data collection for robotic manipulation via compositional generalization, 2024. URL <https://arxiv.org/abs/2403.05110>.
- [16] Joey Hejna, Chethan Bhateja, Yichen Jian, Karl Pertsch, and Dorsa Sadigh. Re-Mix: Optimizing Data Mixtures for Large Scale Imitation Learning. In *Conference on Robot Learning (CoRL)*, 2024.
- [17] Yingdong Hu, Fanqi Lin, Pingyue Sheng, Chuan Wen, Jiacheng You, and Yang Gao. Data scaling laws in imitation learning for robotic manipulation, 2025. URL <https://arxiv.org/abs/2410.18647>.
- [18] Physical Intelligence, Kevin Black, Noah Brown, James Darpinian, Karan Dhabalia, Danny Driess, Adnan Esmail, Michael Equi, Chelsea Finn, Niccolo Fusai, Manuel Y. Galliker, Dibya Ghosh, Lachy Groom, Karol Hausman, Brian Ichter, Szymon Jakubczak, Tim Jones, Liyiming Ke, Devin LeBlanc, Sergey Levine, Adrian Li-Bell, Mohith Mothukuri, Suraj Nair, Karl Pertsch, Allen Z. Ren, Lucy Xiaoyang Shi, Laura Smith, Jost Tobias Springenberg, Kyle Stachowicz, James Tanner, Quan Vuong, Homer Walke, Anna Walling, Haohuan Wang, Lili Yu, and Ury Zhilinsky. $\pi_{0.5}$: a vision-language-action model with open-world generalization, 2025. URL <https://arxiv.org/abs/2504.16054>.
- [19] Physical Intelligence, Kevin Black, Noah Brown, James Darpinian, Karan Dhabalia, Danny Driess, Adnan Esmail, Michael Equi, Chelsea Finn, Niccolo Fusai, et al. $\pi_{0.5}$: a Vision-Language-Action Model with Open-World Generalization. In *Conference on Robot Learning (CoRL)*, 2025.
- [20] Simar Kareer, Dhruv Patel, Ryan Punamiya, Pranay Mathur, Shuo Cheng, Chen Wang, Judy Hoffman, and Danfei Xu. Egomimic: Scaling imitation learning via egocentric video. In *2025 IEEE International Conference on Robotics and Automation (ICRA)*, pages 13226–13233, 2025. doi: 10.1109/ICRA55743.2025.11127989.
- [21] Alexander Khazatsky, Karl Pertsch, Suraj Nair, Ashwin Balakrishna, Sudeep Dasari, Siddharth Karamcheti, Soroush Nasiriany, Mohan Kumar Srirama, Lawrence Yunliang Chen, Kirsty Ellis, et al. DROID: A Large-Scale In-the-Wild Robot Manipulation Dataset. In *Proceedings of Robotics: Science and Systems (RSS)*, 2024.
- [22] Moo Jin Kim, Karl Pertsch, Siddharth Karamcheti, Ted Xiao, Ashwin Balakrishna, Suraj Nair, Rafael Rafailov, Ethan Foster, Grace Lam, Pannag Sanketi, Quan Vuong, Thomas Kollar, Benjamin Burchfiel, Russ Tedrake, Dorsa Sadigh, Sergey Levine, Percy Liang, and Chelsea Finn. OpenVLA: An Open-Source Vision-Language-Action Model. In *Conference on Robot Learning (CoRL)*, 2024.
- [23] Marion Lepert, Ria Doshi, and Jeannette Bohg. Shadow: Leveraging segmentation masks for cross-embodiment policy transfer, 2025. URL <https://arxiv.org/abs/2503.00774>.
- [24] Marion Lepert, Jiaying Fang, and Jeannette Bohg. Masquerade: Learning from in-the-wild human videos using data-editing, 2025. URL <https://arxiv.org/abs/2508.09976>.
- [25] Vincent Liu, Ademi Adeniji, Haotian Zhan, Siddhant Haldar, Raunaq Bhirangi, Pieter Abbeel, and Lerrel Pinto. Egozero: Robot learning from smart glasses, 2025. URL <https://arxiv.org/abs/2505.20290>.
- [26] Yangcen Liu, Woo Chul Shin, Yunhai Han, Zhenyang Chen, Harish Ravichandar, and Danfei Xu. Immimic: Cross-domain imitation from human videos via mapping and interpolation, 2025. URL <https://arxiv.org/abs/2509.10952>.
- [27] Ajay Mandlekar, Soroush Nasiriany, Bowen Wen, Iretiayo Akinola, Yashraj Narang, Linxi Fan, Yuke Zhu, and Dieter Fox. MimicGen: A Data Generation System for Scalable Robot Learning using Human Demonstrations. In *Conference on Robot Learning (CoRL)*, 2023.
- [28] Soroush Nasiriany, Abhiram Maddukuri, Lance Zhang, Adeet Parikh, Aaron Lo, Abhishek Joshi, Ajay Mandlekar, and Yuke Zhu. RoboCasa: Large-Scale Simulation of Everyday Tasks for Generalist Robots. In *Proceedings of Robotics: Science and Systems (RSS)*, 2024.
- [29] NVIDIA, :, Johan Bjorck, Fernando Castañeda, Nikita Cherniadev, Xingye Da, Runyu Ding, Linxi "Jim" Fan, Yu Fang, Dieter Fox, Fengyuan Hu, Spencer Huang, Joel Jang, Zhenyu Jiang, Jan Kautz, Kaushil Kundalia, Lawrence Lao, Zhiqi Li, Zongyu Lin, Kevin Lin, Guilin Liu, Edith Llontop, Loic Magne, Ajay Mandlekar, Avnish Narayan, Soroush Nasiriany, Scott Reed, You Liang Tan, Guanzhi Wang, Zu Wang, Jing Wang, Qi Wang, Jiannan Xiang, Yuqi Xie, Yinzhen Xu, Zhenjia Xu, Seonghyeon Ye, Zhiding Yu, Ao Zhang, Hao Zhang, Yizhou Zhao, Ruijie Zheng, and Yuke Zhu. Gr00t n1: An open foundation model for generalist humanoid robots, 2025. URL <https://arxiv.org/abs/2503.14734>.
- [30] Abby O’Neill, Abdul Rehman, Abhinav Gupta, Abhiram Maddukuri, Abhishek Gupta, Abhishek Padalkar, Abraham Lee, Acorn Pooley, Agrim Gupta, Ajay Mandlekar, et al. Open X-Embodiment: Robotic Learning Datasets and RT-X Models. In *International Conference on Robotics and Automation (ICRA)*, 2024.
- [31] Maximus A. Pace, Prithwish Dan, Chuanruo Ning, Atiksh Bhardwaj, Audrey Du, Edward W. Duan, Wei-Chiu Ma, and Kushal Kedia. X-diffusion: Training

- diffusion policies on cross-embodiment human demonstrations, 2025. URL <https://arxiv.org/abs/2511.04671>.
- [32] Omar Rayyan, John Abanes, Mahmoud Hafez, Anthony Tzes, and Fares Abu-Dakka. Mv-umi: A scalable multi-view interface for cross-embodiment learning, 2025. URL <https://arxiv.org/abs/2509.18757>.
- [33] Modi Shi, Li Chen, Jin Chen, Yuxiang Lu, Chiming Liu, Guanghui Ren, Ping Luo, Di Huang, Maoqing Yao, and Hongyang Li. Is diversity all you need for scalable robotic manipulation?, 2025. URL <https://arxiv.org/abs/2507.06219>.
- [34] Andrew Szot, Bogdan Mazouze, Omar Attia, Aleksei Timofeev, Harsh Agrawal, Devon Hjelm, Zhe Gan, Zsolt Kira, and Alexander Toshev. From Multimodal LLMs to Generalist Embodied Agents: Methods and Lessons. In *Conference on Computer Vision and Pattern Recognition (CVPR)*, 2025.
- [35] Gemini Robotics Team, Saminda Abeyruwan, Joshua Ainslie, Jean-Baptiste Alayrac, Montserrat Gonzalez Arenas, Travis Armstrong, Ashwin Balakrishna, Robert Baruch, Maria Bauza, Michiel Blokzijl, et al. Gemini Robotics: Bringing AI into the Physical World. *arXiv preprint arXiv:2503.20020*, 2025.
- [36] Yuqi Wang, Xinghang Li, Wenxuan Wang, Junbo Zhang, Yingyan Li, Yuntao Chen, Xinlong Wang, and Zhaoxiang Zhang. Unified vision-language-action model, 2025. URL <https://arxiv.org/abs/2506.19850>.
- [37] Youguang Xing, Xu Luo, Junlin Xie, Lianli Gao, Hengtao Shen, and Jingkuan Song. Shortcut learning in generalist robot policies: The role of dataset diversity and fragmentation, 2025. URL <https://arxiv.org/abs/2508.06426>.
- [38] Yashuai Yan, Esteve Valls Mascaro, and Dongheui Lee. Imitationnet: Unsupervised human-to-robot motion re-targeting via shared latent space, 2024. URL <https://arxiv.org/abs/2309.05310>.
- [39] Jonathan Yang, Catherine Glossop, Arjun Bhorkar, Dhruv Shah, Quan Vuong, Chelsea Finn, Dorsa Sadigh, and Sergey Levine. Pushing the Limits of Cross-Embodiment Learning for Manipulation and Navigation. In *Proceedings of Robotics: Science and Systems (RSS)*, 2024.
- [40] Jonathan Heewon Yang, Dorsa Sadigh, and Chelsea Finn. Polybot: Training One Policy Across Robots While Embracing Variability. In *Conference on Robot Learning (CoRL)*, 2023.
- [41] Chengbo Yuan, Rui Zhou, Mengzhen Liu, Yingdong Hu, Shengjie Wang, Li Yi, Chuan Wen, Shanghang Zhang, and Yang Gao. Motiontrans: Human vr data enable motion-level learning for robotic manipulation policies, 2025. URL <https://arxiv.org/abs/2509.17759>.

VIII. ADDITIONAL SIMULATION DETAILS

A. Training Data

We collect data on 10 different scenes with 3 different robots (UR5e, Kinova, Franka) on an Omron base. Each (robot, scene) pair has 50 different trajectories. For task and trajectory pairing, we choose 3 more scenes to collect 50 more trajectories each per robot in order to have enough data after filtering. For each state, we collect 3 different observations at randomized camera angles in order to achieve diversity in the perspective axis.

Evaluation Tasks

For our simulation evaluation, we focus on two primary pick-and-place tasks drawn from RoboCasa-X: *PnP Counter*→*Sink* and *PnP Sink*→*Counter*. We adapt these tasks slightly so that their object sets, layouts, and camera viewpoints are compatible with our real-world setups while preserving the core semantics of the original benchmarks. All tasks use a fixed third-person camera view of a single kitchen layout to facilitate consistent cross-embodiment comparisons.

PnP Counter→**Sink**. As in RoboCasa-X, the robot must pick up an object from the countertop and place it anywhere inside the sink. In our variant, we limit the number of object categories to four and adjust the region from which the objects are initialized on the counter to avoid degenerate configurations (e.g., objects starting too close to the sink or outside the reachable workspace).

PnP Sink→**Counter**. This task mirrors the reverse direction: the robot picks an object from the sink and places it on a plate positioned to the right of the sink. We use a single object category for this task to reduce ambiguity in the goal state and to align closely with our real-world evaluation protocol.

IX. ADDITIONAL REAL-WORLD DETAILS

Robot Platforms

Our real-world experiments utilize four distinct robotic platforms to evaluate cross-embodiment translation:

- **Franka Emika Panda**: 7-DOF robotic arm with parallel-jaw gripper, workspace radius of approximately 85cm, and 6-axis force/torque sensor for contact sensing.
- **WidowX-250**: 6-DOF robotic arm manufactured by Trossen Robotics with parallel-jaw gripper, more compact workspace compared to Franka, and lower payload capacity (750g).
- **PiperX**: Compact desktop manipulator with 6-DOF and parallel-jaw end-effector, designed for tabletop manipulation tasks with high precision but limited reach.

Robot Controllers

We use the DROID codebase [21] as our main wrapper for robot control, integrating platform-specific control interfaces for each robotic system:

- **Franka Emika Panda**: Controlled via the DROID dataset which provides real-time Cartesian and joint-space control with an impedance controller.

- **WidowX-250**: Utilizes the official WidowX SDK from Trossen Robotics, providing direct servo control and position feedback through the onboard microcontroller.
- **PiperX**: Controlled through CAN bus communication, enabling precise joint-level control with real-time feedback from embedded encoders.

The DROID wrapper standardizes the control interface across all platforms, handling trajectory execution, safety monitoring, and data logging consistently regardless of the underlying hardware control method.

Task Descriptions

We focus on two primary manipulation tasks that require precise control and can be standardized across different robot platforms:

- **Pen in Cup**: The robot must pick up a pen from a tabletop surface and place it vertically into a designated cup. This task requires precise grasping, trajectory planning to avoid collisions, and accurate placement with proper orientation.
- **Book on Bookshelf**: The robot must grasp a book lying flat on a table and place it vertically on a bookshelf slot. This task tests the ability to handle larger objects, manage different grasp poses, and execute placement with spatial precision.

A. Scenes

In order to ensure that the scenes collected in the training dataset do not lead to data leakage during evaluation, we collect data in 2 different locations—one for training and one for evaluation. While both are indoor environments, evaluation is done in a kitchen-like setting.

Data Collection Protocol

For real-world data collection, we follow a standardized protocol to ensure consistency:

- 1) **Environment Setup**: Each task is performed in a controlled tabletop environment with consistent lighting conditions. Objects are placed in predetermined positions marked by subtle visual cues to ensure repeatability.
- 2) **Demonstration Collection**: Human demonstrators operate each robot using teleoperation to collect successful task demonstrations. We collect 50 demonstrations per robot for each task, ensuring diverse approach strategies while maintaining task success.
- 3) **Cross-Robot Pairing**: For trajectory-paired data, we collect demonstrations of the same task instance (identical object placement and goal configuration) across different robots. These paired demonstrations are then temporally aligned using Dynamic Time Warping (DTW) on end-effector trajectories.
- 4) **Viewpoint Variation**: Third-person cameras are positioned at multiple angles and heights to capture diverse viewpoints. Each robot setup includes both fixed third-person and wrist-mounted cameras.



Fig. 10. **Simulation Robots.** Simulation robots with diverse camera angles and objects on a countertop scene.



Fig. 11. **Real Robots.** Real robots with diverse camera angles and objects on a kitchen scene for the pen in cup task.

5) **Appearance Augmentation:** To increase visual diversity without requiring extensive real-world data collection, we employ DALL-E 3 for inpainting robot appearances while preserving scene context. This allows us to simulate different robot textures and colors within the same task episodes. The prompt we use is "Change the color of the robot with a different texture"

1) *OXE Dataset Mixture:* The following table shows the data mixture for the OXE data:

Dataset	Split
Bridge	12.5%
DROID	12.5%
Fractal	12.5%
Taco Play	12.5%
Jaco Play	12.5%
Roboturk	12.5%
NYU Door Opening	12.5%
Viola	12.5%

TABLE I
DATA SPLITS

2) *Data Loading:* We load all datasets through the LeRobot format, using the Open-X Embodiment (OXE) `repo_id` as the primary entry point for each source. Each

dataset is first converted into a standardized LeRobot schema that exposes RGB images, proprioception, actions, and task prompts under a common set of keys. We then apply dataset-specific *repacking transforms* to map raw fields (e.g., joint positions, gripper states, multi-view camera streams) into this unified interface before feeding them to the Pi0.5 data pipeline.

For each embodiment, we reuse precomputed normalization statistics (means and variances) stored as dataset assets, ensuring consistent scaling across sources. The data pipeline composes three stages of transforms: (1) *repack transforms* that remap dataset-specific keys into a common observation/action structure, (2) *data transforms* that apply embodiment-specific preprocessing (e.g., converting absolute to delta joint actions, adapting ALOHA or DROID conventions to Pi0.5), and (3) *model transforms* that resize images, tokenize the language prompt, and pad action/state sequences to match the model’s action horizon. This design lets us train on heterogeneous LeRobot datasets without ad hoc sharding logic or manual trajectory slicing while keeping the alignment between observation and action spaces explicit.

3) *Model Training:* We fine-tune a Pi0.5-style VLA model on our compositional cross-embodiment dataset using the OpenPI training stack. Concretely, we begin from a Pi0.5 base checkpoint and perform LoRA-style low-rank adaptation on the vision-language backbone and action head while freezing

the remaining weights. This yields a memory- and compute-efficient training setup that preserves the base model’s broad visual-language competence while specializing a relatively small number of parameters for cross-embodiment translation.

We co-fine-tune jointly on target and translation data, sampling batches with a 50:50 ratio between target episodes and source episodes drawn from the OXE+Translational mixture. Inside the OXE + Translational Mixture, we also weight the data by 50:50 when applicable (leading to a 25%, 25%, 50% split between OXE, translational, and target data).

TABLE II
Pi0.5 LORA TRAINING HYPERPARAMETERS. TYPICAL VALUES USED
 ACROSS OUR EXPERIMENTS.

Hyperparameter	Value
Base model	Pi0.5 VLA
Fine-tuning strategy	Full
Batch size (global)	32
Optimizer	AdamW
Learning rate schedule	Cosine decay with warmup
Peak learning rate	5×10^{-5}
Warmup steps	10,000
Max token length	180 (single-arm)
Weight decay	10^{-2}
Target:source sampling ratio	50:50

X. EXPERIMENT TABLES

Table 1: Coverage vs. Pairing Results (Figure 1)

Key findings: Target-only baseline: 35.0%; Target upper bound: 75.0%. For morphology, target-only performance is 24.0%. Trajectory pairing consistently outperforms other strategies, with diverse coverage being most effective for viewpoint and appearance domains.

Table 2: Comparison with Open-Source Datasets (Figure 2)

Key findings: Our OXE+Translational approach consistently outperforms all baselines, with particularly large gains on complex manipulation tasks like Flip Mug (35-40 percentage point improvements over baseline).

Table 3: Real-World Transfer Results (Figure 4)

Key findings: Real-world results confirm simulation trends, with OXE+Translational achieving 25-35 percentage point improvements over baselines. The method is robust across different robot morphologies and task complexities.

Table 4: Scaling Analysis Summary (Figure 3)

Key findings: Viewpoint and appearance benefits scale smoothly with diversity, while morphology shows saturation effects. Trajectory pairing maintains consistent advantages across all scaling levels. Target upper bound: 75.0%.

TABLE III
SUCCESS RATES (%) ACROSS COVERAGE AND PAIRING STRATEGIES FOR DIFFERENT DOMAIN SHIFTS. RESULTS SHOW MEAN \pm 95% CI OVER 100 SIMULATION TRIALS.

Domain	Coverage	Unpaired	Task-Paired	Trajectory-Paired
Viewpoint	Targeted	45.0 \pm 3.0	50.0 \pm 3.0	52.0 \pm 3.0
	Diverse	64.0 \pm 3.0	68.0 \pm 3.0	70.0 \pm 3.0
Morphology	Targeted	24.0 \pm 4.0	46.0 \pm 4.0	62.0 \pm 4.0
	Diverse	28.0 \pm 4.0	48.0 \pm 4.0	64.0 \pm 4.0
Appearance	Targeted	48.0 \pm 2.5	55.0 \pm 2.5	57.0 \pm 2.5
	Diverse	54.0 \pm 2.5	62.0 \pm 2.5	68.0 \pm 2.5

TABLE IV
SUCCESS RATES (%) COMPARING OUR COMPOSITIONAL APPROACH WITH LARGE-SCALE OPEN-SOURCE TRAINING. RESULTS FOR PANDA AND JACO TARGET ROBOTS ACROSS FOUR SIMULATION TASKS.

Task	Robot	Baseline	Bridge+DROID	OXE	OXE+Translational
PnP Counter→Sink	Panda	18.0 \pm 2.5	18.0 \pm 2.6	23.0 \pm 3.0	40.0 \pm 3.1
	Jaco	12.0 \pm 2.5	18.0 \pm 2.6	22.0 \pm 3.0	38.0 \pm 3.1
PnP Sink→Counter	Panda	16.0 \pm 2.5	24.0 \pm 2.6	27.0 \pm 3.0	39.0 \pm 3.1
	Jaco	10.0 \pm 2.5	24.0 \pm 2.6	26.0 \pm 3.0	36.0 \pm 3.1
Flip Mug	Panda	22.0 \pm 2.5	28.0 \pm 2.6	33.0 \pm 3.0	68.0 \pm 3.1
	Jaco	20.0 \pm 2.5	28.0 \pm 2.6	32.0 \pm 3.0	62.0 \pm 3.1
Open Cabinet	Panda	34.0 \pm 2.5	35.0 \pm 2.6	40.0 \pm 3.0	55.0 \pm 3.1
	Jaco	28.0 \pm 2.5	35.0 \pm 2.6	38.0 \pm 3.0	56.0 \pm 3.1

TABLE V
REAL-WORLD SUCCESS RATES (%) ACROSS DIFFERENT ROBOT TRANSFER PAIRS. RESULTS AVERAGED OVER 5 SEEDS WITH 95% CONFIDENCE INTERVALS.

Task	Transfer	Baseline	Bridge+DROID	OXE	OXE+Translational
Pen in Cup	PiperX→WidowX	50 \pm 3.5	60 \pm 3.0	65 \pm 3.0	85 \pm 3.0
	WidowX→Franka	40 \pm 4.0	50 \pm 3.5	50 \pm 3.0	75 \pm 3.0
	WidowX→Piper	55 \pm 3.5	65 \pm 3.5	65 \pm 3.0	90 \pm 3.0
Book on Bookshelf	PiperX→WidowX	25 \pm 2.5	35 \pm 3.0	40 \pm 3.0	65 \pm 3.0
	WidowX→Franka	20 \pm 3.0	30 \pm 3.0	35 \pm 3.0	60 \pm 3.0
	WidowX→Piper	30 \pm 2.5	40 \pm 3.0	45 \pm 3.5	65 \pm 3.5

TABLE VI
PERFORMANCE SCALING WITH SOURCE DIVERSITY. SHOWS SUCCESS RATES AT DIFFERENT NUMBERS OF SOURCE EMBODIMENTS/VIEWPOINTS/SCENES FOR EACH METHOD.

Domain	Method	Baseline	2	5	10	20	40
Viewpoint	Naive (Uniform)		45.0	48.0	52.0	58.0	60.0
	Targeted Coverage	35.0	50.0	57.0	61.0	66.0	68.0
	Trajectory-Paired		52.0	61.0	66.0	71.0	74.0
Morphology	Naive (Uniform)		24.0	25.5	28.0	—	—
	Targeted Coverage	24.0	46.0	46.8	48.0	—	—
	Trajectory-Paired		62.0	62.8	64.0	—	—
Appearance	Naive (Uniform)		48.0	50.0	54.0	58.0	60.0
	Targeted Coverage	35.0	55.0	58.0	62.0	66.0	68.0
	Trajectory-Paired		57.0	61.0	66.0	70.0	72.0